

# An Open-Source Numerical Model for Mitigating Refractory Alloy Hot Cracking Susceptibility

Jeffrey W. Sowards, Andrew O'Connor, Fredrick N. Michael, Carly J. Romnes,  
Fernando Reyes Tirado, Omar Mireles

Marshall Space Flight Center



# Outline



- Problem & Motivation
- Background on the Model and Algorithm
- Algorithm Verification vs Past Aluminum Alloy Studies
- Algorithm Verification vs Past Refractory Alloys Weldability Data
- Extrapolations to Refractory-Interstitial (O,C,N) Binary Alloys
- Extending the Approach for Development of Hot Cracking Susceptibility Equations

# Background on Refractory Metals



- Refractory metals and alloys are used for service in extreme high temperature environments:

- Reaction Control System (RCS) thrusters
- Space Nuclear Propulsion (SNP) clad and structure
- Hypergolic / green propulsion chambers and catalyst
- Electric propulsion grids
- Power conversion system heat pipes and regenerators
- Hypersonic wing leading edges



Apollo CSM RCS using C103.  
Courtesy Aerojet-Rocketdyne



TZM alloy heat pipe.  
Courtesy Advanced Cooling Technologies.

Base	Name	Composition (wt%)
Nb	Nb	Nb
	Nb-1Zr	Nb-1Zr
	C103	Nb-10Hf-1Ti
	C129Y	Nb-10Hf-10W-0.1Y
	Cb752	Nb-10W-2.5Zr
	C3009	Nb-30Hf-10W
	WC3015	Nb-28Hf-13W-5Ti-2Ta-1Zr
Mo	FS85	Nb-28Ta-10W-1Zr
	Mo	Mo
	Mo-21Re	Mo-21Re
	Mo-41Re	Mo-41Re
	Mo-44Re	Mo-44Re
	Mo-47.5Re	Mo-47.5Re
W	TZM	Mo-0.5Ti-0.08-Zr-0.2C
	Mo	Mo
W	W	W
	W-25Re	W-25Re
Ta	Ta	Ta
	Ta-10W	Ta-10W
Ir	Ir	Ir
	DOP26	DOP26
Re	Re	Re

Traditional Refractory Alloys



X-51A hypersonic test vehicle. Courtesy USAF.

# Problem and Goal: Fabricating Refractory Alloys



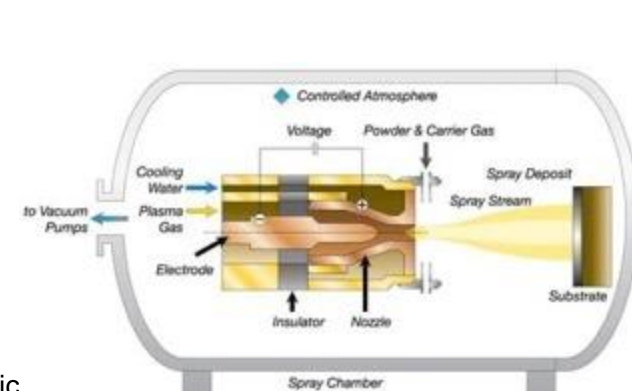
- Typically exhibit poor weldability. Existing alloys were design 60+ years ago and never optimized to be weldable and printable.
  - Thermal shock (thermal stress builds due to extreme high melting point)
  - Brittleness at room temperature (due to shift of ductile to brittle transition)
  - **Solidification cracking (due to segregation of alloying elements and wide solidification temperature ranges induced by alloying)**
- Traditional refractory manufacture is difficult and expensive:
  - Bar, plate, tube, sheet stocks and sizes limited (constrains design)
  - Powder feedstock are angular and not usually alloyed
  - High feedstock cost
  - Relatively difficult to form/machine (fracture prone)
  - Heat treatment requires specialized facilities (O, C, N sensitive)
  - Joining options limited (Usually electron beam welded)
  - Inspection options limited
- Alloys designed for traditional manufacture:
  - Powder metallurgy (CIP, HIP, deposition)
  - Forging
  - Wire and/or plunge EDM
  - W (\$100/kg) or Mo (\$80/kg) alloyed with 25-47.5 wt% Re (\$2.76k/kg) to improve ductility
- **Goal. Develop new refractory alloys using a CALPHAD approach, optimized for printability with L-PBF L-DED and weldability by reducing solidification cracking susceptibility**



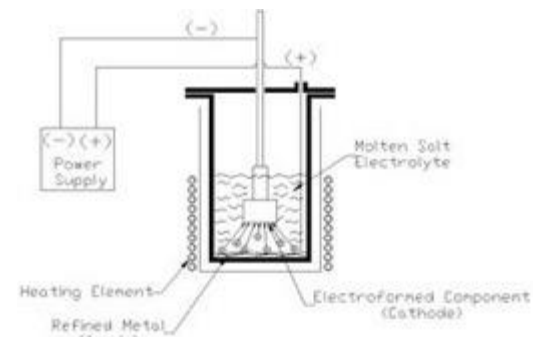
C103 forged bar stock.  
Courtesy ATI.



Hot Isostatic Press (HIP) process [1].



Vacuum Plasma Spray (VPS) process [2].



Electro Deposition / Forming process [3].

[1] <https://www.malvernpanalytical.com/en/industries/advanced-manufacturing/powder-metallurgy/isostatic>

[2] <https://www.neodynamiki.gr/>

[3] <https://plasmapros.com/processes/>

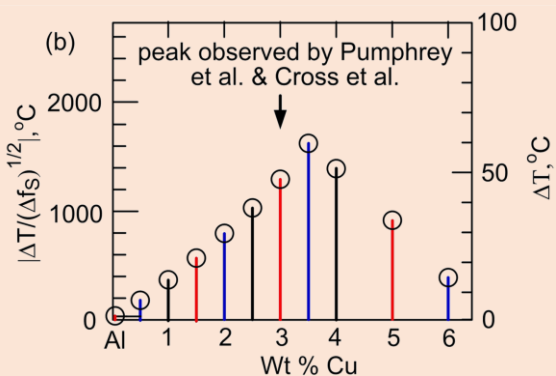
# Model: Kou's Solidification Cracking Criterion



Kou's Cracking Criterion [4]: 
$$\left\{ \begin{array}{l} V_{local} > \phi \sqrt{1 - \beta} \frac{d \sqrt{f_s}}{dT} \frac{dT}{dt} + \phi \frac{d}{dz} [(1 - \sqrt{1 - \beta} \sqrt{f_s}) v_z] \\ \text{(separation)} \quad \text{(growth)} \quad \text{(feeding)} \end{array} \right\}_{\sqrt{f_s} \rightarrow 1}$$

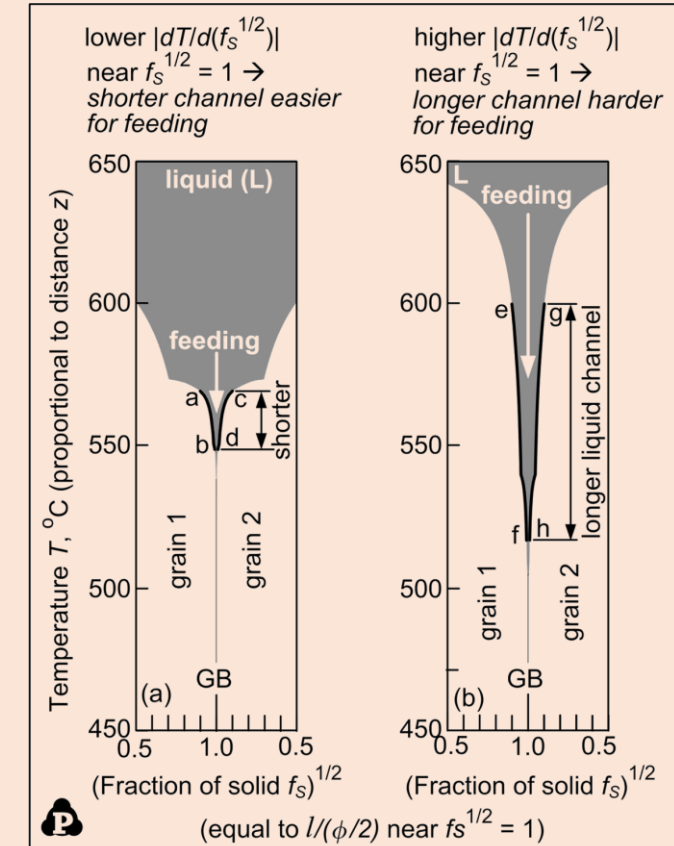
- Considers a balance between grain boundary separation (cracking), lateral growth of grains, and liquid feeding between dendrites
  - $v$  is velocity,  $\phi$  is dendrite diameter,  $\beta$  is shrinkage,  $T$  is temperature,  $f_s$  is fraction solid
- Crack susceptibility increases as  $|dT/d(f_s^{1/2})|$  increases near  $f_s^{1/2} = 1$ .
  - $f_s^{1/2}$  significance is similarity to dimensionless radius of dendrite
  - Steepness of solidification path near terminal solidification results in higher index: suggesting increased crack susceptibility due to slower transverse growth rate and longer passageway for feeding
- Criterion does not predict occurrence but rather susceptibility.
- The Scheil equation is used to predict the solidification path of an alloy, i.e., the plot of  $f_s$  vs  $T$  and usefully couples to this criterion for evaluating influence of composition.

## Composition Influence



[4] Kou. Acta Mat 88 (2015): 366-374  
<https://doi.org/10.1016/j.actamat.2015.01.034>

## Geometrical Significance



# Process Flow and Algorithm to Compute Crack Susceptibility



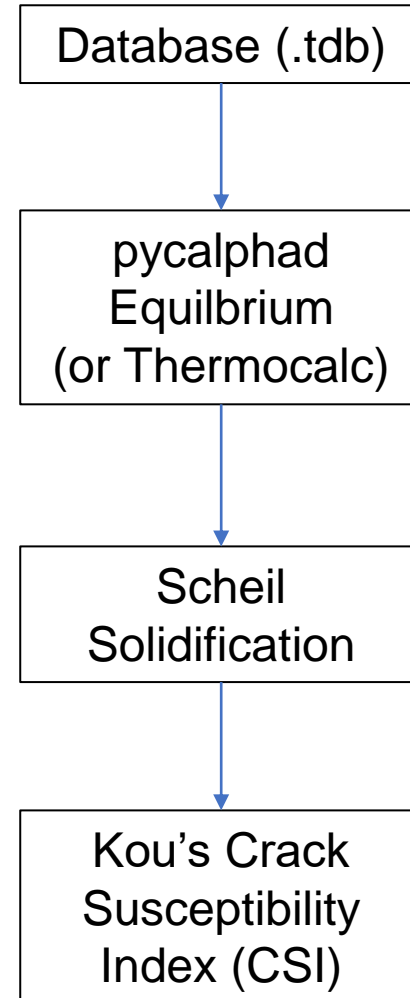
In this work, we numerically implement calculation of Kou's CSI in a Jupyter Notebook with python scripting.

[5] de Walle et al. *Calphad* 61 (2018): 173-178  
<https://avdwgroup.engin.berkeley.edu/>

[6] Otis & Liu. *J. Open Res. Soft.* 5 (2017): 1  
<https://pycalphad.org/>

[7] Bocklund, et al. (2020).  
<https://github.com/pycalphad/scheil>

[4] Kou. *Acta Mat* 88 (2015): 366-374  
<https://doi.org/10.1016/j.actamat.2015.01.034>



## Jupyter Notebook Flow for pycalphad (Python 3)

```
import Dependencies #pycalphad and math packages
Variables = database, elements, phases
Conditions = start_temp, temp_step, filter #Scheil setup
Scheil = T vs fs plot #Calculate
fsnew = sqrt(fs) #take
PowerSmooth = savgol.(T,fsnew) #Savitsky-Golay power smoothing
derivative = abs(gradient(power_smooth) / gradient(fsnew))
Max_value = max(derivative) #between 0.9 and 0.99 fsnew

#Iterate for multiple elements to generate e.g., ternary:
for i in x_element
    for j in y_element
        Perform above

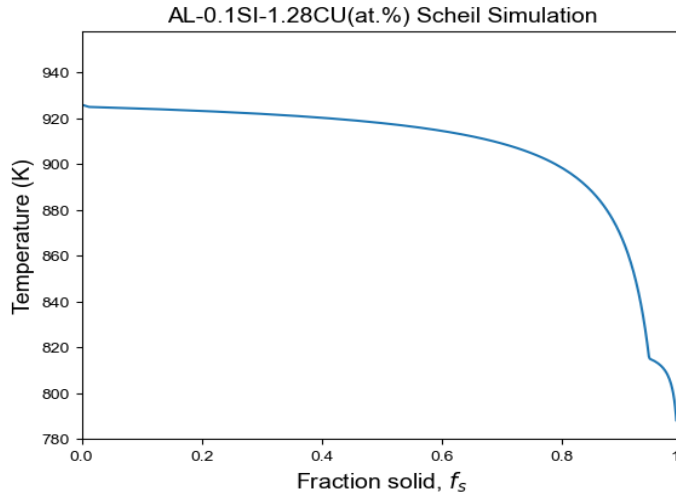
#Log data
#Perform postprocessing and plotting
```

Complete code examples are available in a report online. Plans to post on GitHub.  
[8] Michael & Sowards (2023) NASA-TM-20230002218.  
<https://ntrs.nasa.gov/citations/20230002218>

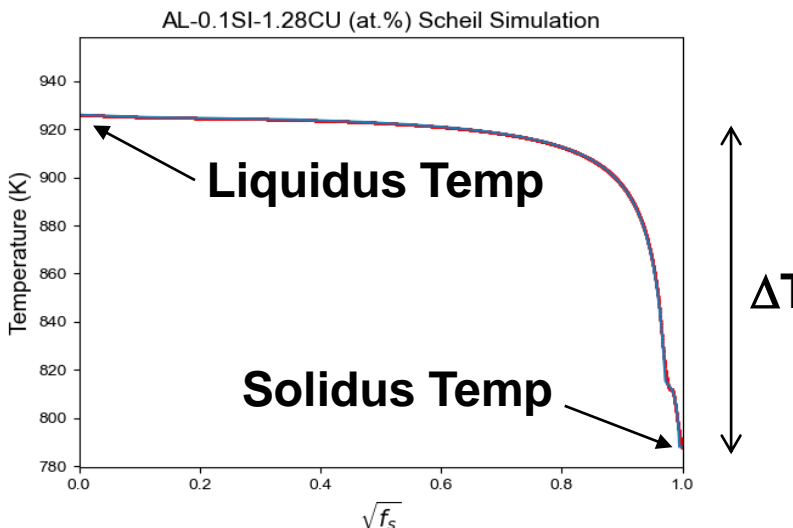
# Example: Jupyter Notebook Output and CSI Calculation



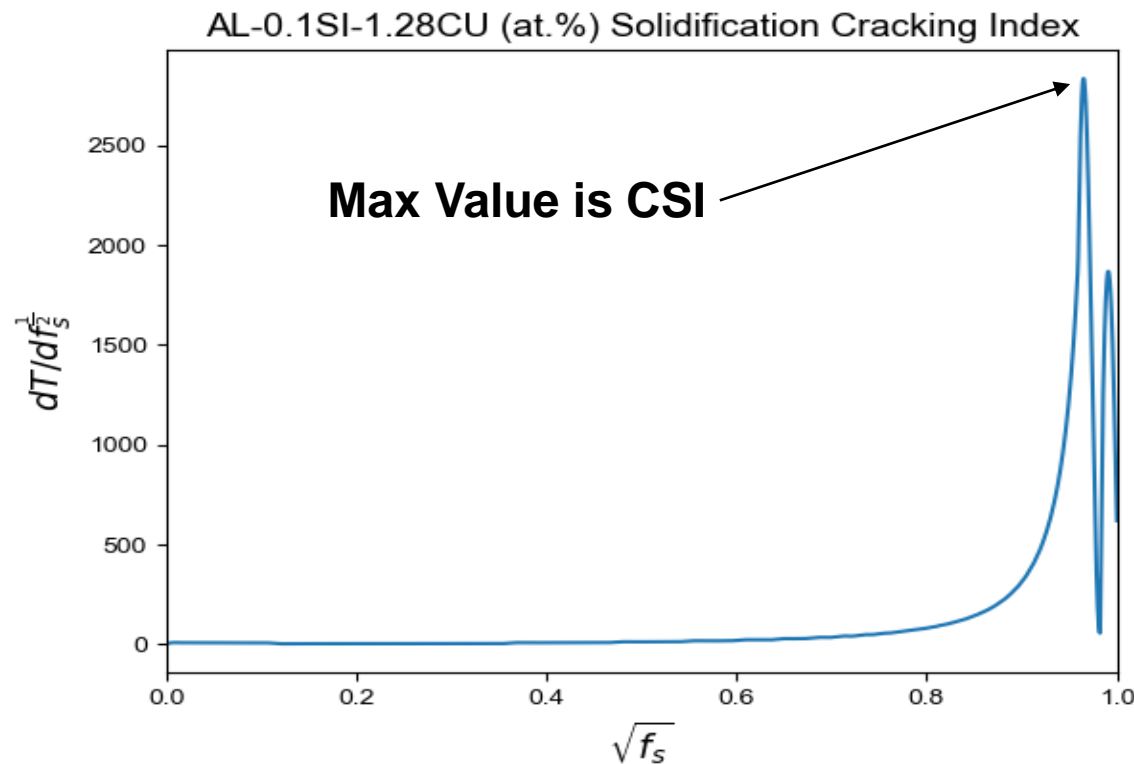
## 1. Compute Scheil Solidification Path



## 2. Perform Best Fit to $f_s^{1/2}$ -T Plot (optional)



## 3. Compute Derivative of $f_s^{1/2}$ -T Best Fit Line



## 4. Find Max CSI and Log Results

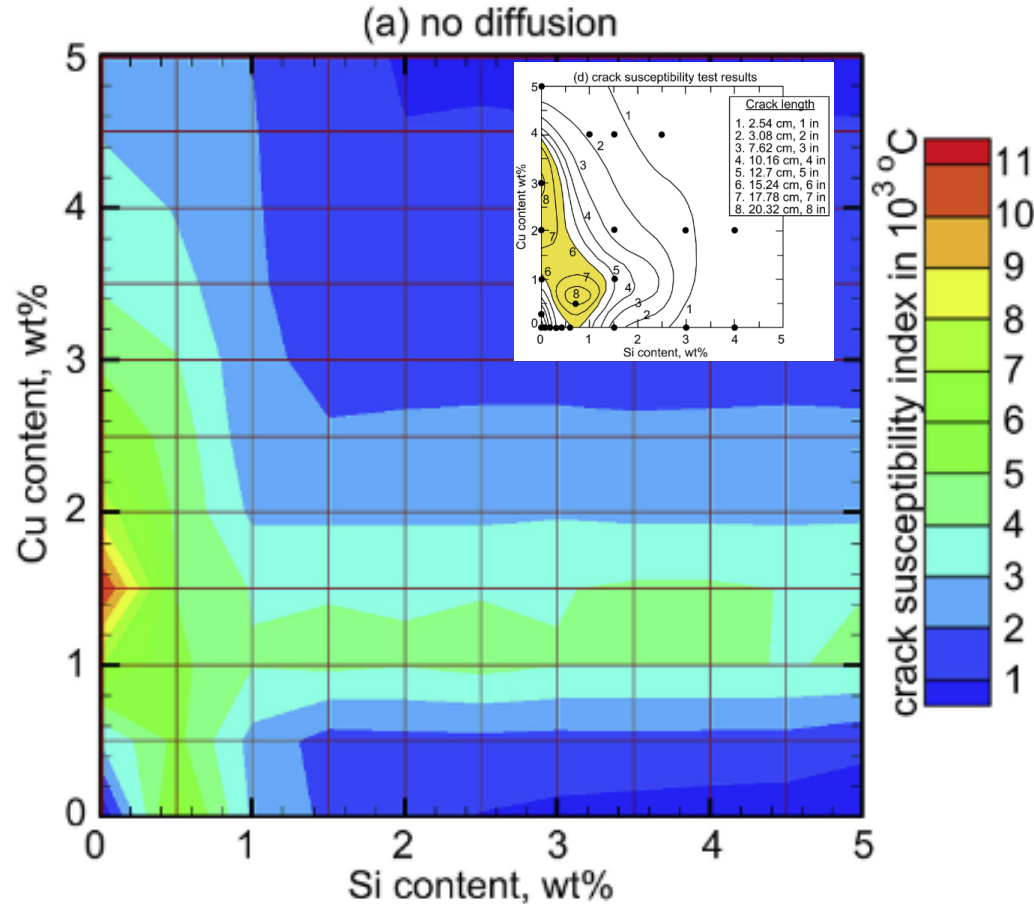
### Jupyter Notebook Output

```
Run # = 18 Total Run time = 166.1 seconds
Composition = {W_SI: 0.001, W_CU: 0.029724137931034483}
Max CSI = 2832.9 K, Max CSI with Filter = 2832.9 K, Solidus Temperature = 788.0 K
```

# Algorithm Verification in Al-Si-Cu Ternary with Open-source Software

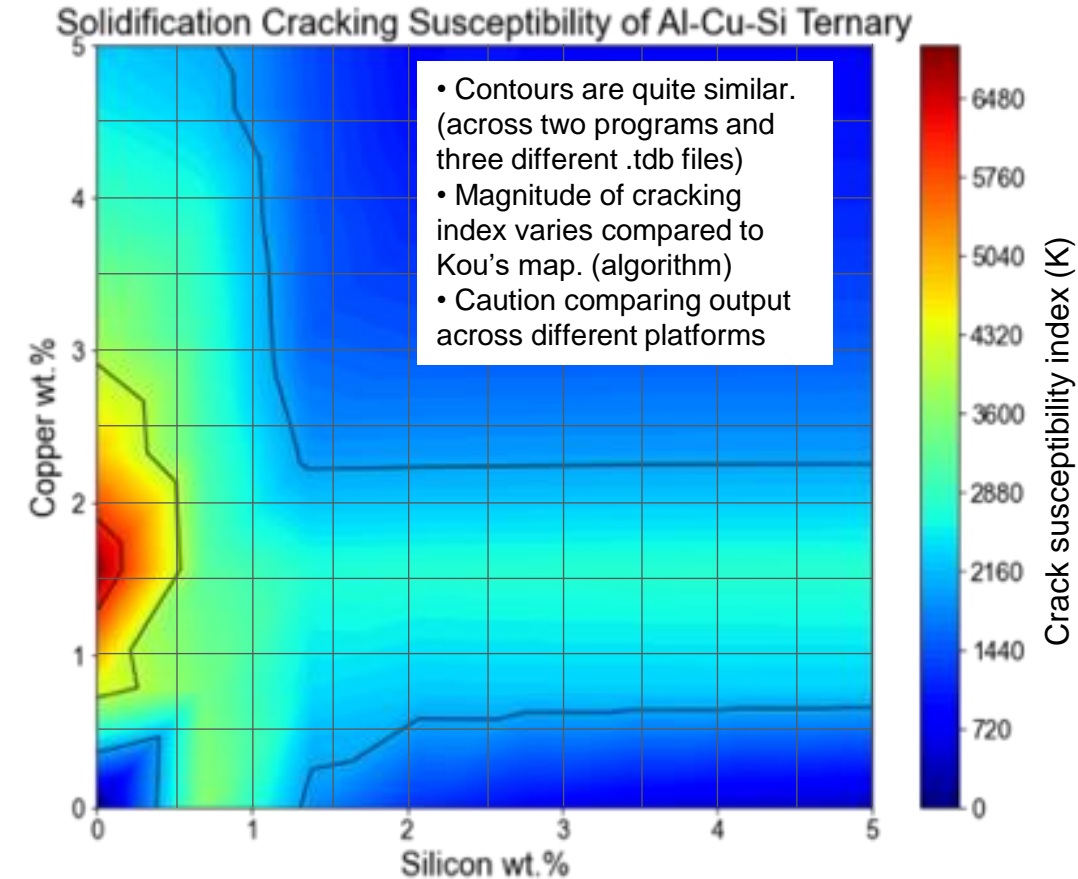


Liu and Kou's Cracking Index Map [9] produced with Pandat + Pan aluminum database. Solidification with no diffusion (Scheil).



[9] Liu and Kou. *Acta Mat.* 125, 15 (2017): 513-523.  
<https://doi.org/10.1016/j.actamat.2016.12.028>

Kou's Cracking Index Map produced with open-source pycalphad + COST507.tdb Solidification with no diffusion (Scheil).



Two open-source TDB were tested producing similar map results:  
[10] Ansara et al. (1998) COST 507.  
[11] Hallstedt et al. *Calphad* 53 (2016): 25-38.

# 1. Algorithm Verification with Refractory Alloy Varestraint Data



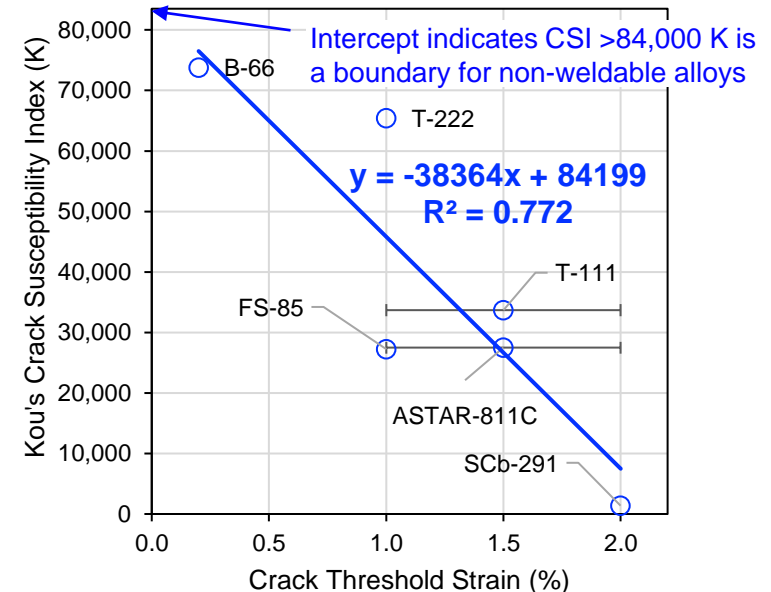
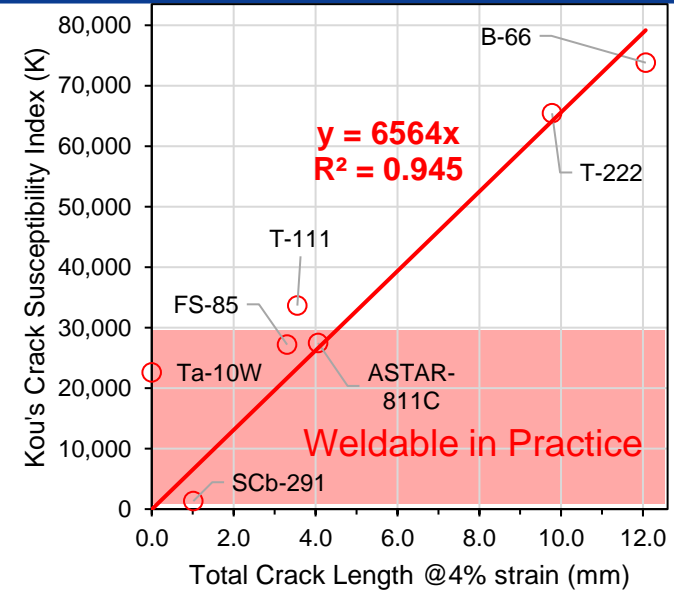
- Lessman and Gold [12] published refractory metal Varestraint testing of seven refractory alloys subject to GTA welding in inert vacuum.

## Refractory Alloy Compositions:

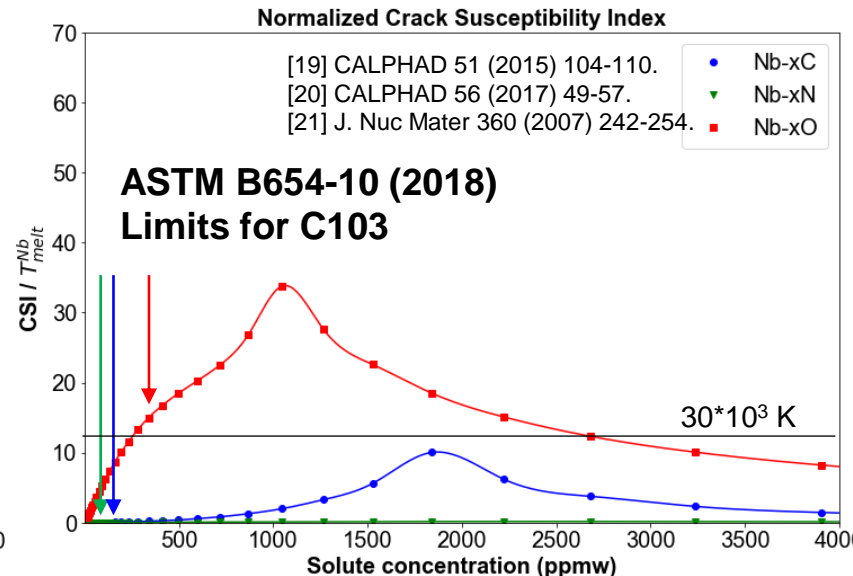
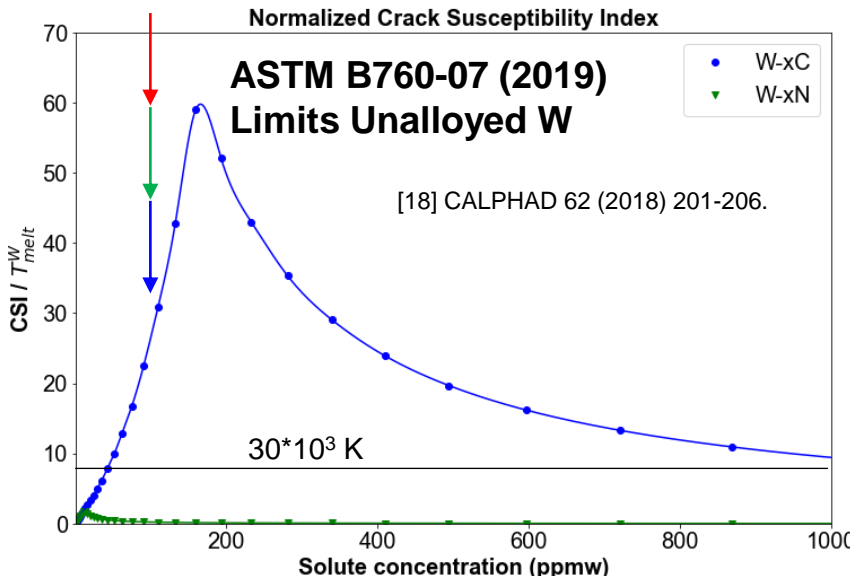
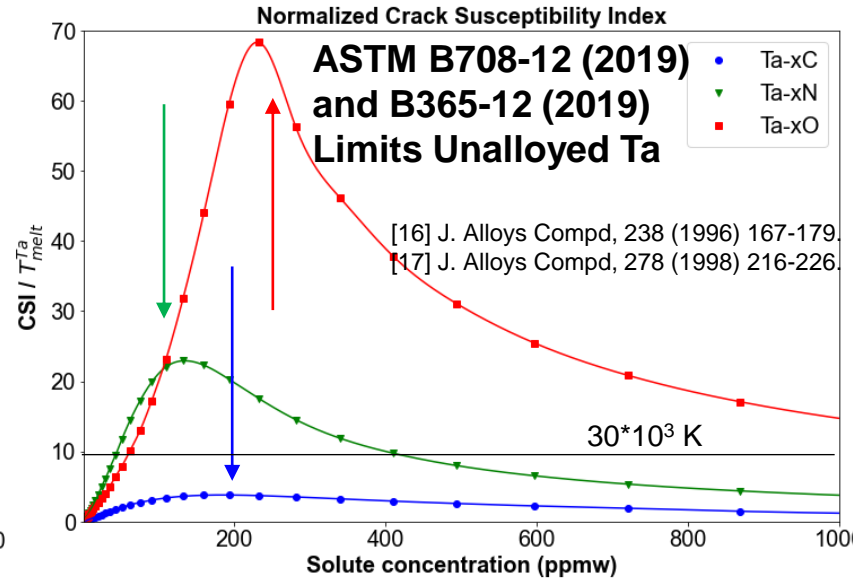
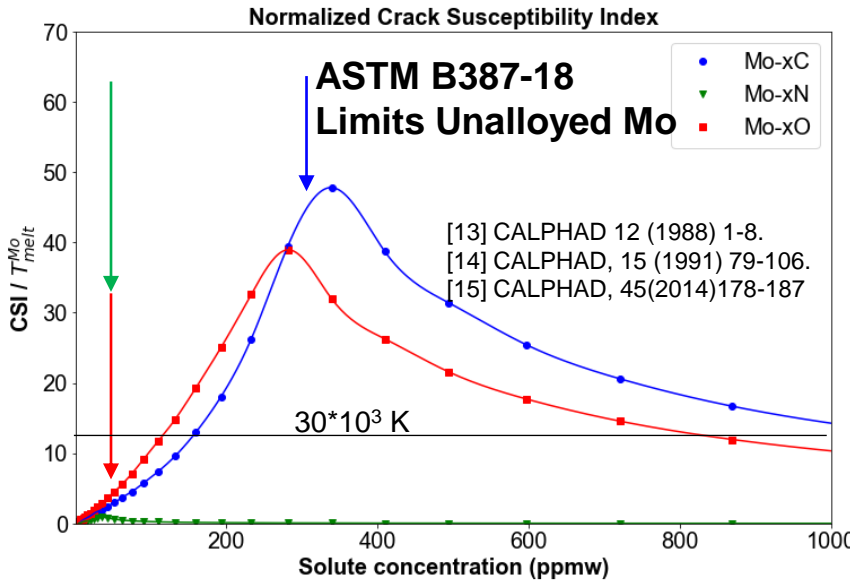
Alloy	Nominal Composition	Ta	Nb	W	Hf	Mo	Re	V	Zr	C ppm	O ppm	N ppm	C ppm	O ppm	N ppm
T-111	Ta-8W-2Hf	balance	-	8.2	2.0	-	-	-	-	40	80	12	33	40	12
ASTAR-811C	Ta-8W-1Re-0.7Hf-0.025C	balance	-	8.1	0.9	-	1.4	-	-	300	70	10	210	5	5
FS-85	Nb-27Ta-10W-1Zr	28.1	balance	10.6	-	-	-	-	0.94	20	90	60	32	53	47
T-222	Ta-9.6W-2.4Hf-0.01C	balance	-	9.2	2.55	-	-	-	-	115	50	20	119	17	11
B-66	Nb-5Mo-5V-1Zr	-	balance	-	-	5.17	-	4.89	1	95	110	63	37	120	70
Ta-10W	Ta-10W	balance	-	9.9	-	-	-	-	-	50	40	20	5	10	10
SCb-291	Nb-10W-10Ta	9.83	balance	10.0	-	-	-	-	-	20	110	40	22	101	20

- Themocalc (TCHEA6.tdb) was used to calculate Scheil solidification paths of those seven alloys and subsequent CSI. Oxygen was **not** in the database.
- CSI shows good correlation to Ta- and Nb-based refractory alloy Varestraint test data.
- Refractory alloys with CSI <  $30 \times 10^3$  K are weldable in practice.
- Refractory alloys with CSI >  $80 \times 10^3$  K would likely crack at all augmented strains.

[12] Lessman and Gold. *Welding J.* (1971): 1s – 8s.



## 2. Crack Susceptibility Index in Binary Refractory Mixtures



- Solidification cracking is strongly influenced by interstitial elements in practice
- CSI of C, N, O interstitial alloys
- CSI is normalized by  $T_{melt}$  for scaling
- Effect of interstitials as follows:

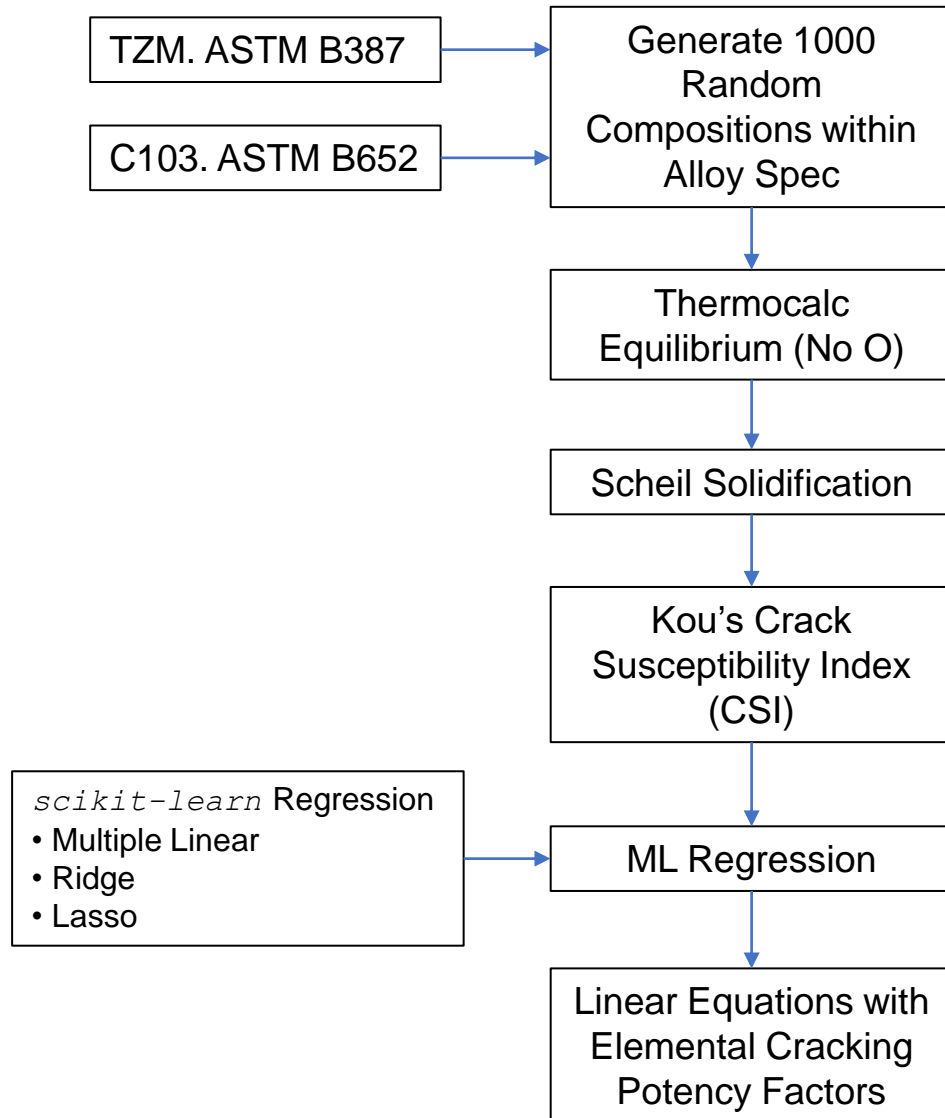
Effect of **Carbon** on CSI:  
 $W > Mo > Ta > Nb$

Effect of **Nitrogen** on CSI:  
 $Ta > Mo > W > Nb$

Effect of **Oxygen** on CSI (No W-O):  
 $Ta > Mo > Nb$

- Comparison to ASTM chemistry limits:
  - Mo: C Limit is near peak CSI
  - Ta: C, N, O limits are near peak CSI
  - W: C limit may be concern, O is unknown
  - Nb: O limit may be concern
- Additive powder recycling pickup of C and O especially will promote cracking.

### 3. Extending the Model: Chemistry-dependent Cracking



Many equations have been developed to relate solidification cracking to alloying elements through multiple linear regression [22].

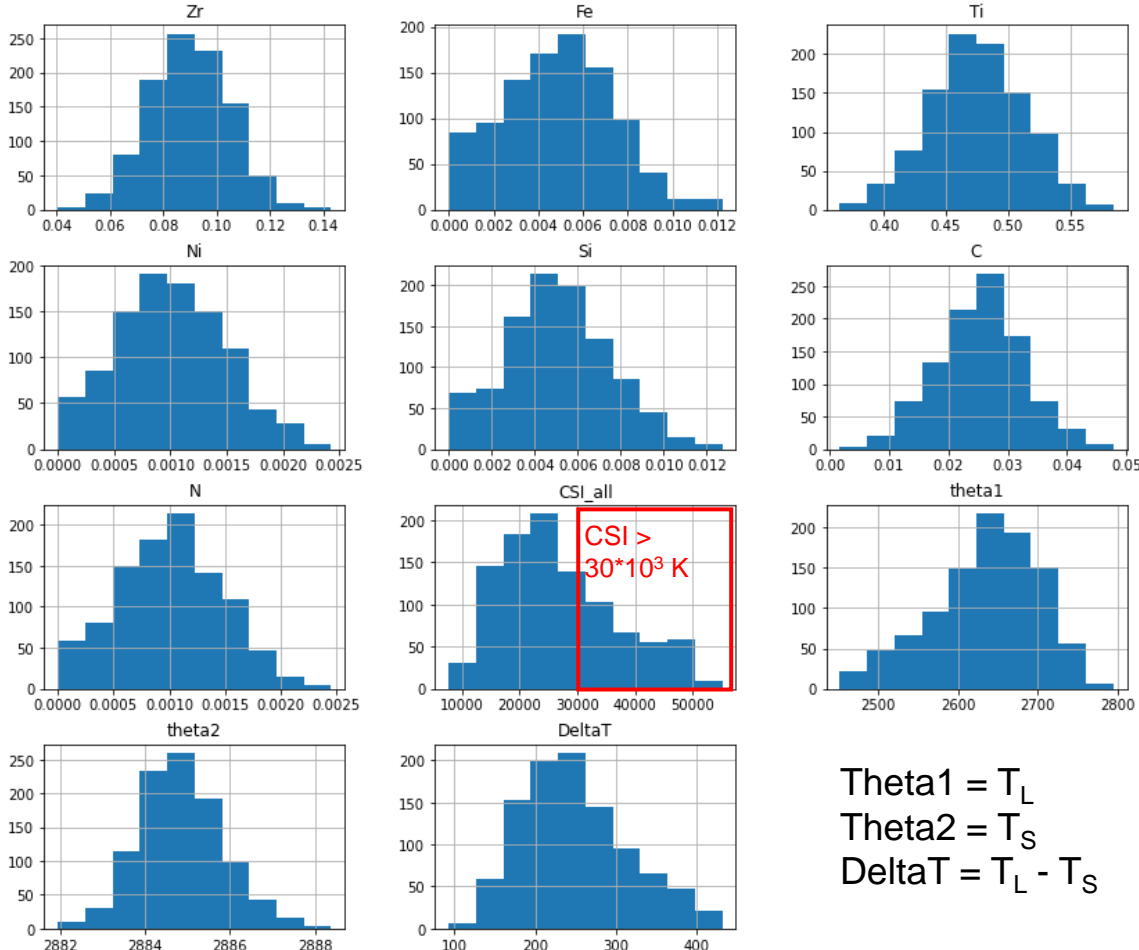
[22] Matsuda (1990). Proc 1<sup>st</sup> US-Japan Symposium on Advances in Welding Metallurgy. 19-36.

Element	TZM Ingot - ASTM B387 (wt.%)	Element	C103 Ingot - ASTM B652 (wt.%)
C	0.01 – 0.04	C	0.015 max
O*	0.003 max	O	0.025 max
N	0.002 max	N	0.010 max
Fe	0.01 max	H	0.0015 max
Ti	0.4 – 0.55	Hf	9 – 11
Si	0.01 max	Ti	0.7 – 1.3
Ni	0.002 max	Zr	0.700 max
Zr	0.06 – 0.12	W	0.500 max
Mo	balance	Ta	0.500 max
*O in powder metallurgy alloy is 0.05 max		Nb	balance

# Input and Results

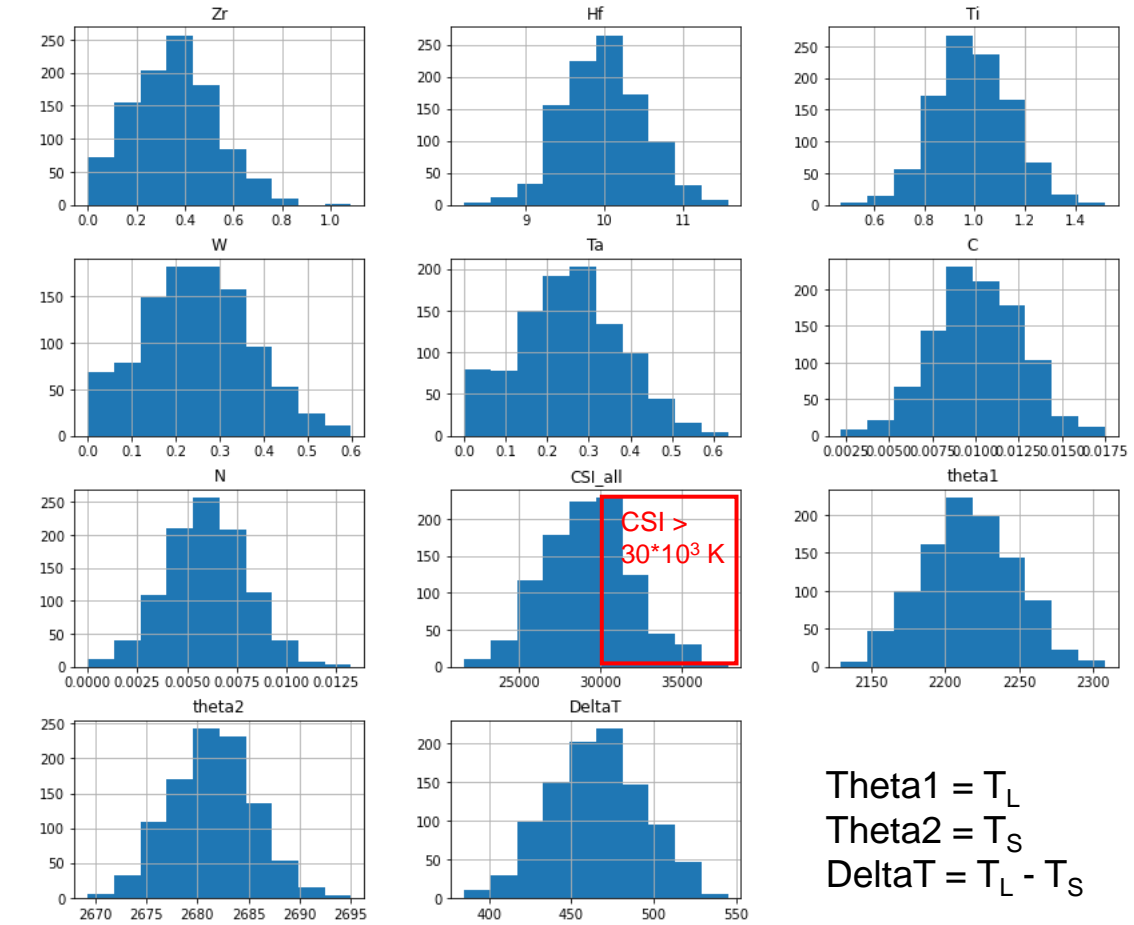


**TZM Distribution  $N = 1,000$**



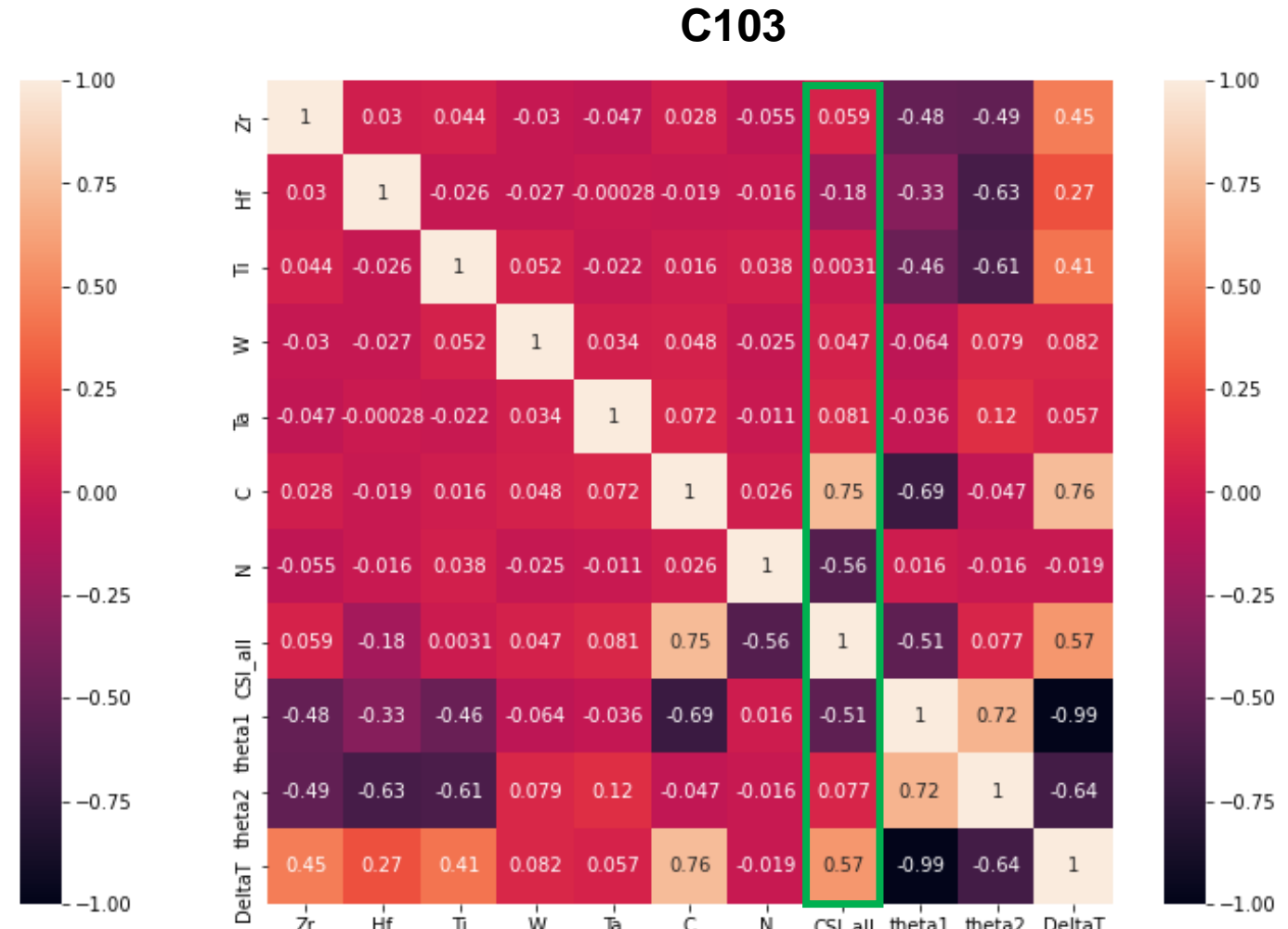
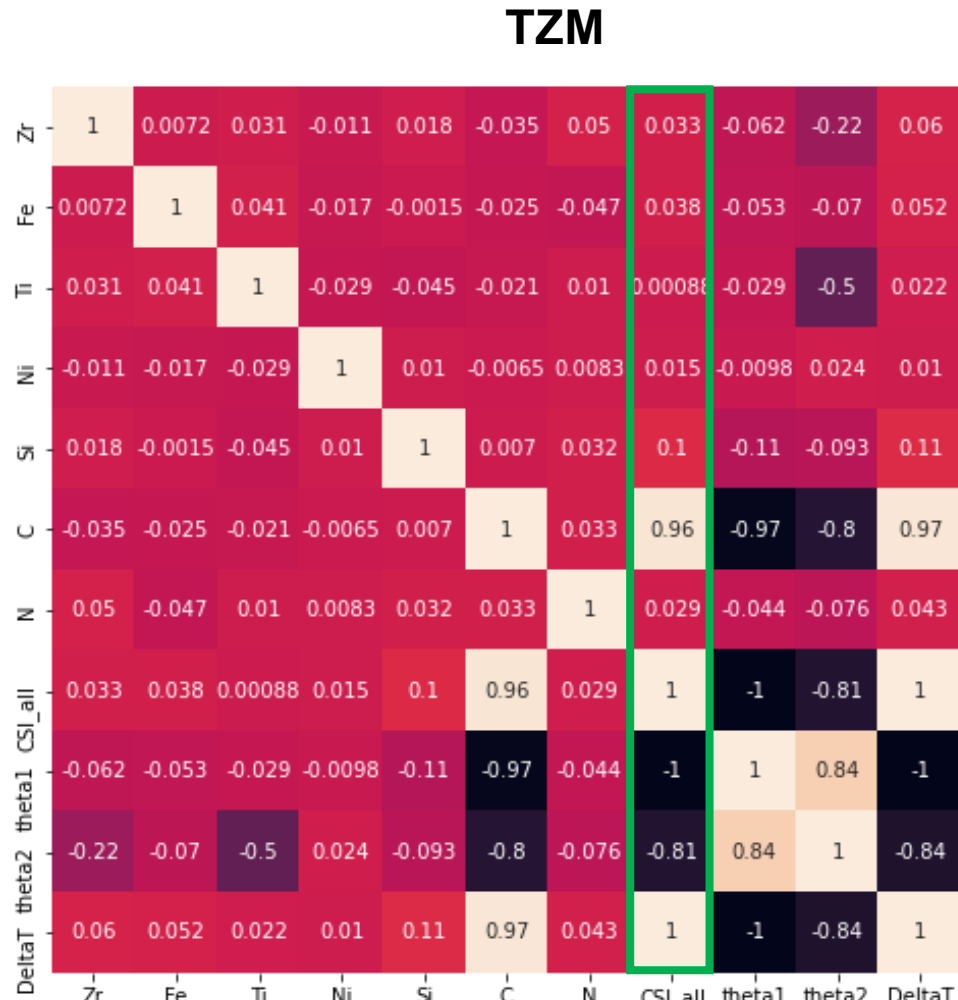
$$\begin{aligned} \text{Theta1} &= T_L \\ \text{Theta2} &= T_S \\ \Delta T &= T_L - T_S \end{aligned}$$

**C103 Distribution  $N = 1,000$**



Negative values of composition are assumed zero. Data are normally distributed. A large portion of compositions produce a  $CSI > 30 \times 10^3$  K.

# Interaction Matrix to Determine Correlations



Multicollinearity (several independent variables are correlated) is not observed.

# Regression Results and Best Fit Model



## TZM

$$\text{CSI} = \beta_0 + \beta_{\text{Zr}}X_{\text{Zr}} + \beta_{\text{Fe}}X_{\text{Fe}} + \beta_{\text{Ti}}X_{\text{Ti}} + \beta_{\text{Ni}}X_{\text{Ni}} + \beta_{\text{Si}}X_{\text{Si}} + \beta_{\text{C}}X_{\text{C}} + \beta_{\text{N}}X_{\text{N}}$$

where X expressed in [wt.%]

Model	Linear	Ridge	Lasso
a	--	0.0001	0.0001
$R^2$	0.94774	0.94768	0.94774
$b_0$	-17066.3	-16805.1	-17065.8
$b_{\text{Zr}}$	43924.2	43753.9	43922.9
$b_{\text{Fe}}$	246464	242320	246450
$b_{\text{Ti}}$	5732.26	5657.58	5731.96
$b_{\text{Ni}}$	465135	325775	464705
$b_{\text{Si}}$	385805	379454	385787
$b_{\text{C}}$	1334869	1332153	1334866
$b_{\text{N}}$	-156242	-105938	-155788

## C103

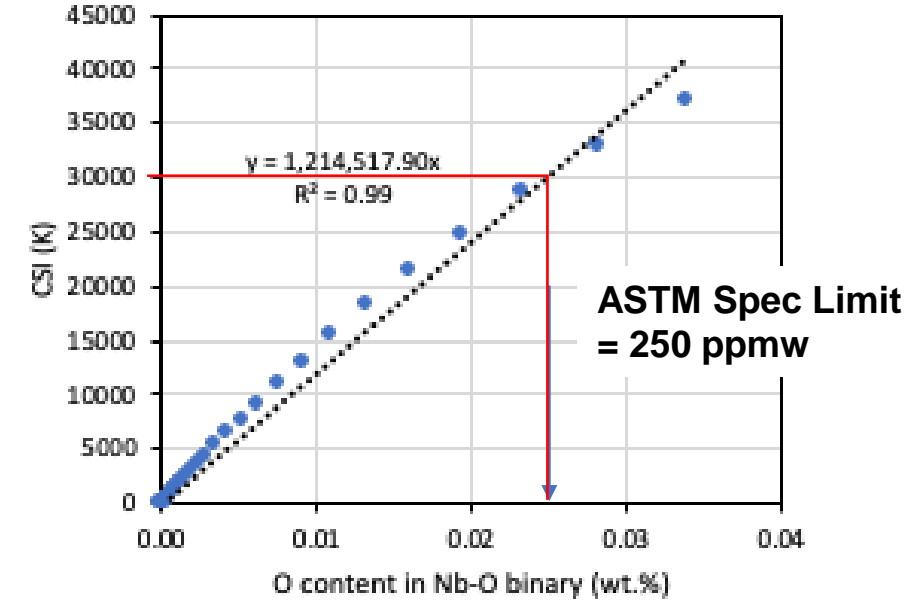
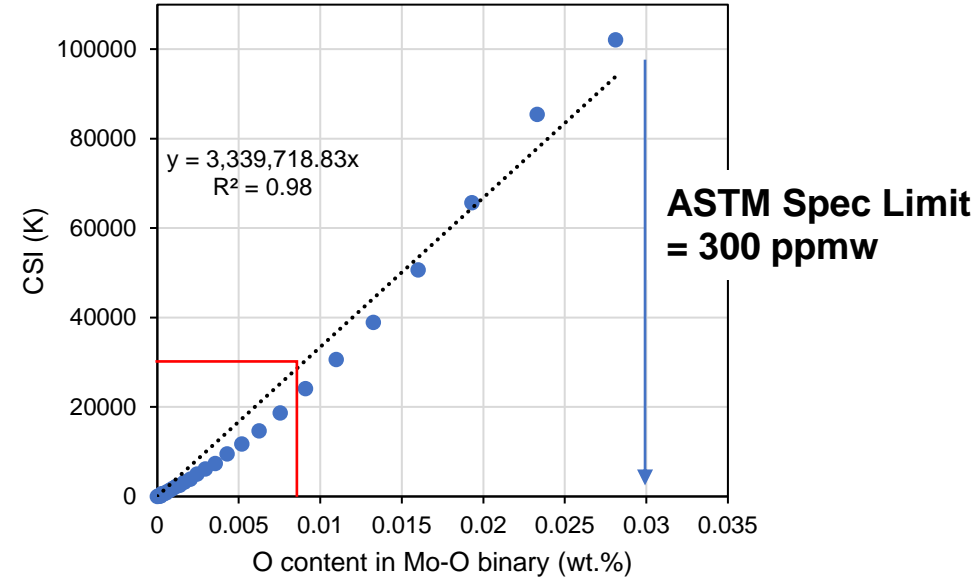
$$\text{CSI} = \beta_0 + \beta_{\text{Zr}}X_{\text{Zr}} + \beta_{\text{Hf}}X_{\text{Hf}} + \beta_{\text{Ti}}X_{\text{Ti}} + \beta_{\text{W}}X_{\text{W}} + \beta_{\text{Ta}}X_{\text{Ta}} + \beta_{\text{C}}X_{\text{C}} + \beta_{\text{N}}X_{\text{N}}$$

where X expressed in [wt.%]

Model	Linear	Ridge	Lasso
a	--	0.0001	0.0001
$R^2$	0.92197	0.92163	0.92197
$b_0$	34966.3	34977.1	34966.3
$b_{\text{Zr}}$	177.93	197.265	177.952
$b_{\text{Hf}}$	-960.084	-960.276	-960.083
$b_{\text{Ti}}$	160.762	153.071	160.747
$b_{\text{W}}$	-208.024	-186.839	-207.989
$b_{\text{Ta}}$	449.447	472.192	449.47
$b_{\text{C}}$	809597	796558	809580
$b_{\text{N}}$	-771158	-752294	-771133

All models produce excellent fits to data. As the alpha value  $\rightarrow 0$ , for Ridge and Lasso the coefficients approached ordinary Least Squares Regression model. Linear multiple regression is selected for further discussion.

# Discussion. Effect of Oxygen



Oxygen was not considered in the complex alloys due to lack of available thermodynamic data for higher order mixtures. The Mo-O and Nb-O binary systems above show that oxygen drastically increases CSI.

We develop a weight factor based on linear interpolation above revealing a weight factor of  $3.34 \times 10^6$  K/[O] and  $1.21 \times 10^6$  K/[O], for Oxygen in TZM and C103, respectively.

# Simplified Linear Models of Elemental Potency on Cracking



Steps:	TZM	C103
1. View Raw CSI coefficients. $X_i$ in [wt. %]	$CSI = -17,066 + 43,924 X_{Zr} + 246,464 X_{Fe} + 5,732 X_{Ti} + 465,135 X_{Ni} + 385,805 X_{Si} + 1,334,869 X_C - 156,242 X_N$	$CSI = 34,966 + 178 X_{Zr} - 960 X_{Hf} + 161 X_{Ti} - 208 X_W + 449 X_{Ta} + 809,597 X_C - 771,158 X_N$
2. Modify with estimated oxygen term based on binary calculation. $X_i$ in [wt. %]	$CSI = -17,066 + 43,924 X_{Zr} + 246,464 X_{Fe} + 5,732 X_{Ti} + 465,135 X_{Ni} + 385,805 X_{Si} + 1,334,869 X_C + 3,339,718 X_O - 156,242 X_N$	$CSI = 34,966 + 178 X_{Zr} - 960 X_{Hf} + 161 X_{Ti} - 208 X_W + 449 X_{Ta} + 809,597 X_C + 1,214,518 X_O - 771,158 X_N$
3. Normalize coefficients by max coefficient (Oxygen in both cases) revealing model with relative potency the alloying elements have on hot cracking susceptibility (HCS)	$HCS = 0.013*Zr + 0.074*Fe + 0.002*Ti + 0.139*Ni + 0.116*Si + 0.4*C + O - 0.047*N$	$HCS = 0.667*C + O - 0.001*Hf - 0.635*N$

- Oxygen and Carbon strongly promote solidification crack susceptibility.
- Nitrogen apparently decreases crack susceptibility especially in C103.
- Fe, Ni, Si promote crack susceptibility in TZM, as do Zr and Ti to lesser extent.

For nominal TZM (Mo-0.475Ti-0.09Zr-0.025C), CSI exceeds  $30 \cdot 10^3$  K at 23 ppmwt O!

For nominal composition of C103 (Nb-10Hf-1Ti), CSI exceeds  $30 \cdot 10^3$  K at 37 ppmwt O!

# Initial validation with Thermo-Calc® databases (TZM)

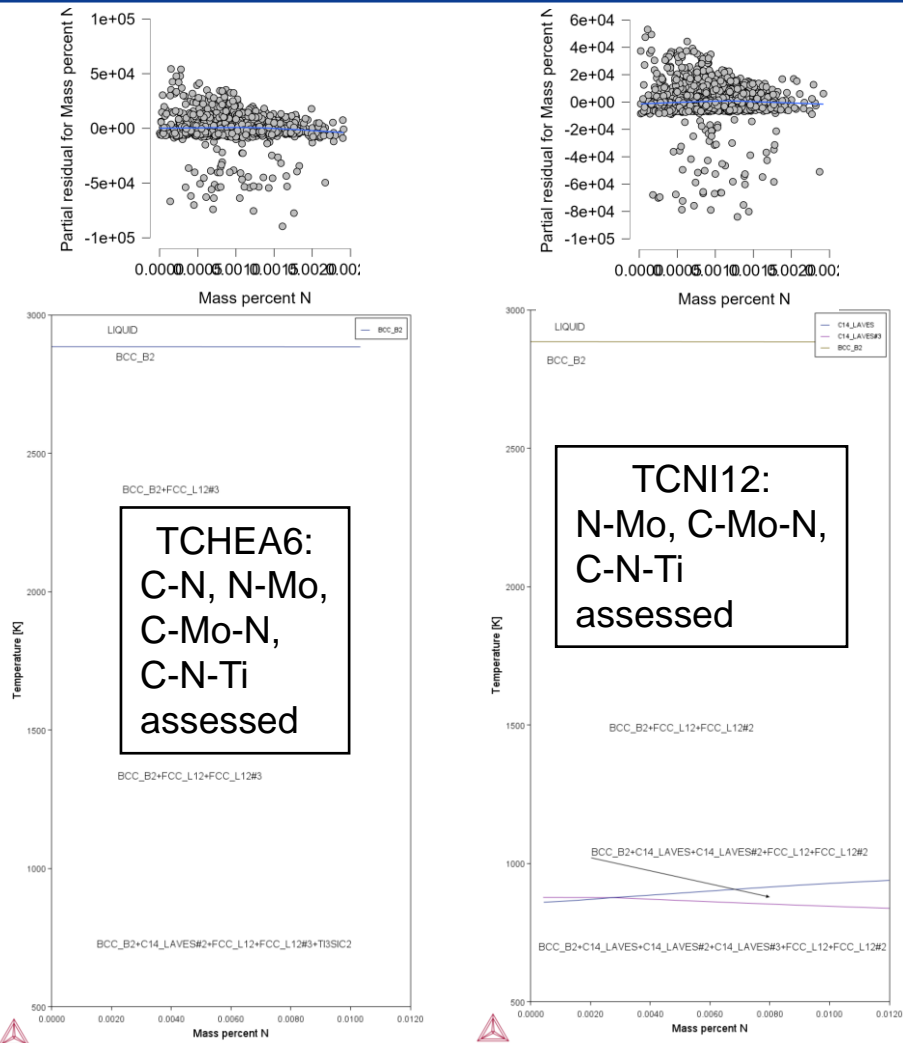


TZM	Database		
	TCHEA6	TCNI12	COST507
$\beta_0$	-13640	-15991	-17066
$\beta_{\text{Zr}}$	125768	71909	43924
$\beta_{\text{Fe}}$	571421	513975	246464
$\beta_{\text{Ti}}$	-6084	20005	5732
$\beta_{\text{Ni}}$	1128000	-5	465135
$\beta_{\text{Si}}$	870811	531083	385805
$\beta_{\text{C}}$	2130000	2049000	1334869
$\beta_{\text{N}}$	-4162300	-27	-156242
$\beta_{\text{O}}$	1400000	1400000	3339719

\*Mo-O for TCHEA6 & TCNI12 calculations taken from TCNI12

Database	Zr	Fe	Ti	Ni	Si	C	O	N
TCNI12	0.051	0.367	0.014		0.379	1.46	1	
COST507	0.013	0.074	0.002	0.139	0.116	0.4	1	-0.047

TZM	Database			
	TCHEA6	TCNI12	COST507	
$\beta_0$				
$\beta_{\text{Zr}}$	0.089834	0.051364	0.013152	
$\beta_{\text{Fe}}$	0.408158	0.367125	0.073798	
$\beta_{\text{Ti}}$	-0.00435	0.014289	0.001716	
$\beta_{\text{Ni}}$	0.805714		0.139274	
$\beta_{\text{Si}}$	0.622008	0.379345	0.11552	
$\beta_{\text{C}}$	1.521429	1.463571	0.399695	
$\beta_{\text{N}}$	-2.97307		-0.04678	
$\beta_{\text{O}}$		1	1	1



Some agreement w.r.t HCS potency from C, N, and O;  
other contributions of Fe, Ni, and Si also notable; TCNI12 closer to COST507

# Initial validation with Thermo-Calc® databases (C103)

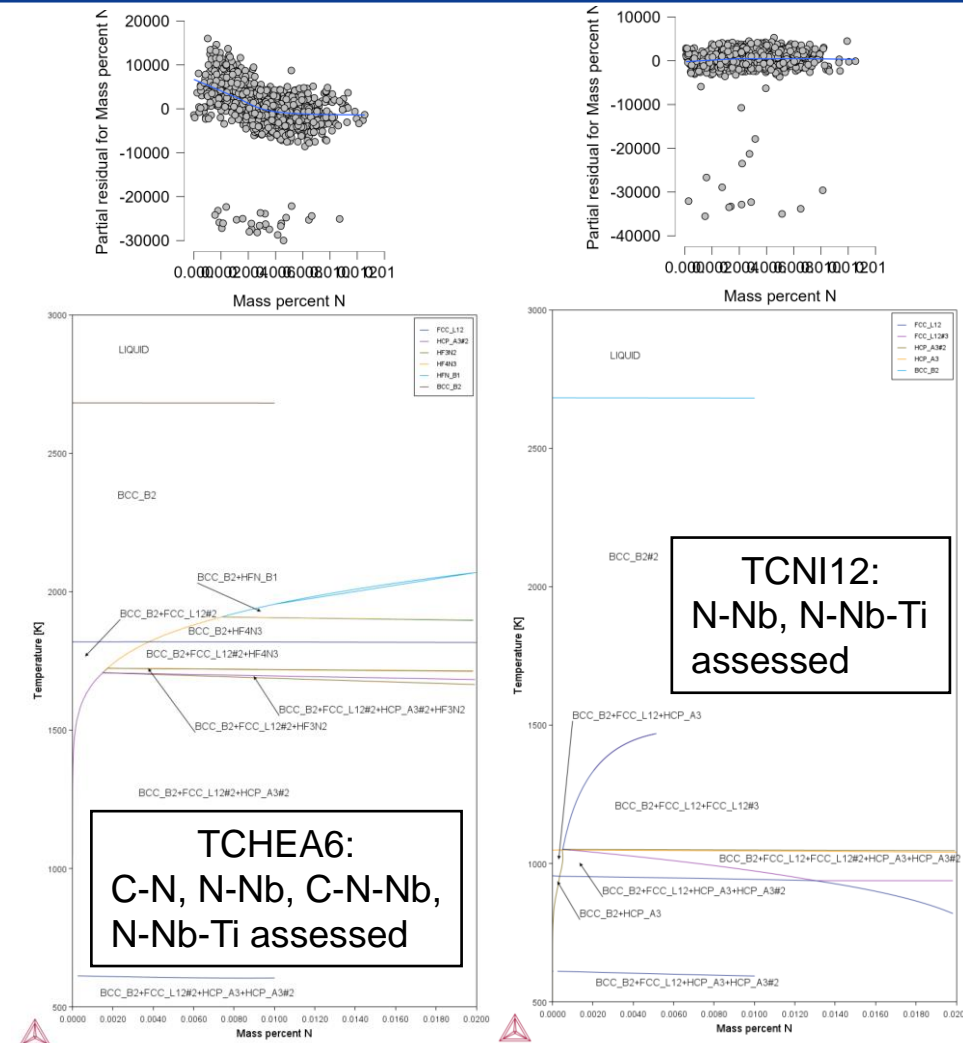


C103	Database		
	TCHEA6	TCNI12	COST507
$\beta_0$	71798.16	36715.06	34966.3
$\beta_{\text{Zr}}$	-433.77	5677.079	177.93
$\beta_{\text{Hf}}$	-3303.51	-1474.5	-960.084
$\beta_{\text{Ti}}$	-5747.47	391.995	160.762
$\beta_{\text{W}}$	-204.478	1285.546	-208.024
$\beta_{\text{Ta}}$	89.486	-1127.69	449.447
$\beta_{\text{C}}$	784781.5	1517000	809597
$\beta_{\text{N}}$	-775735	94119.62	-771158
$\beta_{\text{O}}$	1225000	1225000	1214518

\*Nb-O for TCHEA6 & TCNI12 calculations taken from TCNI12

Database	C	O	Hf	Ti	N
TCHEA6	0.641	1	-0.003	-0.005	-0.633
COST507	0.667	1	-0.001		-0.635

C103	Database		
	TCHEA6	TCNI12	COST507
$\beta_0$			
$\beta_{\text{Zr}}$		0.004634	
$\beta_{\text{Hf}}$	-0.0027	-0.0012	-0.00079
$\beta_{\text{Ti}}$	-0.00469		
$\beta_{\text{W}}$		0.001049	
$\beta_{\text{Ta}}$		-0.00092	
$\beta_{\text{C}}$	0.640638	1.238367	0.666599
$\beta_{\text{N}}$	-0.63325	0.076832	-0.63495
$\beta_{\text{O}}$	1	1	1



Agreement w.r.t HCS potency from C and O; N potency agreement for TCHEA6 & COST507, more confident in TCHEA6 than TCNI12 as C-N-Nb assessed

# Summary



1. A numerical approach was developed to calculate Kou's Solidification Crack Susceptibility Index (CSI) using open-source Python code with both an open-source and a commercial CALPHAD equilibrium solver.
  - The method was verified against previous calculations and aluminum alloy solidification cracking data.
2. The numerical approach was applied to refractory metals, which are inherently difficult to study from a weldability testing standpoint since welding is often done in vacuum.
  - Calculated CSI showed strong empirical correlation to vacuum Varestraint testing of Ta- and Nb-alloys.
  - Correlations indicate that refractory alloys with  $\text{CSI} < 30 \times 10^3 \text{ K}$  are weldable in practice.
3. Calculation of CSI for refractory-interstitial (O,C,N) binary systems revealed ASTM chemistry specs are not ideal for optimal weldability and AM printability.
4. This work revealed the effect of compositional variations on a series of refractory metals and showed the framework defined here will be useful in:
  - The development of new alloys that have improved weldability and AM printability
  - Placing compositional limits on existing alloys
  - Consideration of manufacturing process controls such as powder reuse during 3D printing